Atmos. Chem. Phys. Discuss., 14, 17037–17066, 2014
www.atmos-chem-phys-discuss.net/14/17037/2014/
doi:10.5194/acpd-14-17037-2014

Atmospheric Chemistry and Physics Discussions

Mapping $CH_4 : CO_2$ ratios in Los Angeles with CLARS-FTS from Mount Wilson, California

K. W. Wong[1], D. Fu[1], T. J. Pongetti[1], S. Newman[2], E. A. Kort[4], R. Duren[1], Y.-K. Hsu[3], C. E. Miller[1], Y. L. Yung[2], and S. P. Sander[1]

[1]NASA Jet Propulsion Laboratory, Pasadena, California, USA
[2]California Institute of Technology, Pasadena, California, USA
[3]California Air Resources Board, Sacramento, California, USA
[4]University of Michigan, Ann Arbor, Michigan, USA

Received: 23 May 2014 – Accepted: 8 June 2014 – Published: 26 June 2014

Correspondence to: K. W. Wong (clare.wong@jpl.nasa.gov)

Published by Copernicus Publications on behalf of the European Geosciences Union.

Abstract

The Los Angeles megacity, which is home to more than 40 % of the population in California, is the second largest megacity in the United States and an intense source of anthropogenic greenhouse gases (GHGs). Quantifying GHG emissions from the megacity and monitoring their spatiotemporal trends are essential to be able to understand the effectiveness of emission control policies. Here we measure carbon dioxide (CO_2) and methane (CH_4) across the Los Angeles megacity using a novel approach – ground-based remote sensing from a mountaintop site. A Fourier Transform Spectrometer (FTS) with agile pointing optics, located on Mount Wilson at 1.67 km above sea level, measures reflected near infrared sunlight from 29 different surface targets on Mount Wilson and in the Los Angeles megacity to retrieve the slant column abundances of CO_2, CH_4 and other trace gases above and below Mount Wilson. This technique provides persistent space and time resolved observations of path-averaged dry-air GHG concentrations, XGHG, in the Los Angeles megacity and simulates observations from a geostationary satellite. In this study, we combined high sensitivity measurements from the FTS and the panorama from Mount Wilson to characterize anthropogenic CH_4 emissions in the megacity using tracer : tracer correlations. During the period between September 2011 and October 2013, the observed $XCH_4 : XCO_2$ excess ratio, assigned to anthropogenic activities, varied from 5.4 to 7.3 ppb CH_4 $(\text{ppm } CO_2)^{-1}$, with an average of 6.4 ± 0.5 ppb CH_4 $(\text{ppm } CO_2)^{-1}$ compared to the value of 4.6 ± 0.9 ppb CH_4 $(\text{ppm } CO_2)^{-1}$ expected from the California Air Resources Board (CARB) bottom-up emission inventory. Persistent elevated $XCH_4 : XCO_2$ excess ratios were observed in Pasadena and in the eastern Los Angeles megacity. Using the FTS observations on Mount Wilson and the bottom-up CO_2 emission inventory, we derived a top-down CH_4 emission of 0.39 ± 0.06 Tg CH_4 year^{-1} in the Los Angeles megacity. This is 18–61 % larger than the state government's bottom-up CH_4 emission inventory and consistent with previous studies.

ACPD
14, 17037–17066, 2014

1 Introduction

The Los Angeles megacity – a sprawling urban expanse of ∼ 100 km × 100 km and 15 million people – covers only ∼ 4 % of California's land area but is home to more than 43 % of its population and dominates the state's anthropogenic greenhouse gas (GHG) emissions. By treating the megacity as an effective "point source", we can quantify trends in this critical component of the state's GHG emissions and support California's goal of reducing GHG emissions to the 1990 level by 2020 mandated by the state's The Global Warming Solutions Act of 2006 (AB32).

Emissions of carbon dioxide (CO_2) and methane (CH_4) in the Los Angeles megacity originate largely from different economic sectors and are expected to have distinctly different spatial and temporal patterns. Anthropogenic CO_2 is derived mainly from motor vehicle exhaust (Transportation), exhibiting strong diurnal variability and weak seasonal variability, and from natural gas fueled power plants (Power) with a few large stationary emitters and significant seasonal variability. Overall CO_2 emissions for transportation and power plants are known to within ±10 % from fuel usage and emission factors. On the other hand, the CH_4 emissions budget is highly uncertain and contains significant but poorly quantified emissions from a variety of sources such as landfills and wastewater treatment plants (Waste), oil and gas production, storage and delivery infrastructure (Power and Residential), dairy farms (Agriculture) and geologic seeps (Geology). Recent studies estimating CH_4 emissions from atmospheric observations have shown that the bottom-up total CH_4 emissions inventory in the Los Angeles megacity have uncertainties of 30 % to > 100 % (Wunch et al., 2009; Hsu et al., 2010; Wennberg et al., 2012; Jeong et al., 2013; Peischl et al., 2013). Atmospheric observations may be used to characterize spatial and temporal patterns in CO_2 and CH_4 within the Los Angeles megacity and to provide initial estimates of sectoral emissions attribution.

Wunch et al. (2009) demonstrated the estimation of GHGs using the ground-based column measurements acquired at a Total Carbon Column Observing Network (TCCON) station in Pasadena, California, in the Los Angeles basin. Since column

ACPD
14, 17037–17066, 2014

measurements are relatively insensitive to boundary layer height variations and are less influenced by local sources than ground in situ measurements, they should be more representative of the area. They reported that the bottom-up CH_4 emissions for the Los Angeles megacity are less than half of the top-down CH_4 emissions. The large uncertainty in the bottom-up CH_4 emission inventory in the Los Angeles megacity has also been supported by the CH_4 : CO_2 ratios observed by aircraft campaigns, ARCTAS-CARB in 2008 and CalNex in 2010 (Wennberg et al., 2012; Peischl et al., 2013), and in-situ observations on Mount Wilson (Hsu et al., 2010).

Despite the potential of atmospheric observations to quantify the emissions of CH_4, CO_2 and other GHGs in the Los Angeles megacity, they have certain limitations for tracking long-term GHG emissions. Kort et al. (2013) showed that surface in situ observations from no single site within or adjacent to the Los Angeles megacity accurately capture the emissions from the entire region. Similarly, ground-based total column measurements from Pasadena also lack sensitivity to emissions from across the entire region. Kort et al. (2013) concluded that the size and complexity of the Los Angeles megacity urban dome requires a network of at least eight strategically located continuous surface in situ observing sites to quantify and track GHG emissions over time. However, this minimum network would have limited capabilities to identify and isolate emissions from specific sectors and/or localized sources. It is therefore necessary to develop a robust, long-term measurement solution, which resolves emissions the Los Angeles megacity both spatially and temporally.

The present study reports GHG measurements of the Los Angeles megacity from an elevated vantage point, the California Laboratory for Atmospheric Remote Sensing (CLARS), located on Mt Wilson 1670 m a.s.l. and overlooking the Los Angeles megacity (Fig. 1). We present column averaged dry air mole fraction CO_2 (XCO_2) and CH_4 (XCH_4) measurements for 29 reflection points distributed across Los Angeles. The measurements cover daylight hours for the two-year period between 2011 and 2013. We determine the enhancements in XCH_4 and XCO_2 in the basin compared to background levels, and use the spatial distribution of correlations in

ACPD
14, 17037–17066, 2014

XCH_4(excess) : XCO_2(excess) ratio to quantify emissions in the megacity. We compare our results to column, surface in-situ and aircraft in situ observations and compare our derived megacity CH_4 emissions estimates with the results from previous studies.

CLARS provides a unique long-term data record that simulates geostationary (GEO) satellite observations for the Los Angeles basin. CLARS maps the diurnal variability of both XCO_2 and XCH_4 within the Los Angeles urban dome with hourly time scales. It has functioned operationally since 2011, and its sustained measurements are yielding insights into the scientific value of GEO GHG monitoring, as well as helping to define GEO-based GHG measurement requirements. Existing and future satellite instruments such as TES (AURA), TANSO-FTS (GOSAT), and OCO-2, all sample from sun-synchronous low-earth orbits. These platforms sample globally, but return to the same measurement point on the Earth infrequently, with repeat cycles ranging from days to weeks. In contrast, GEO measurements, such as those from the proposed Geostationary Fourier Transform Spectrometer (GEO-FTS), map the complete field of regard with high spatial resolution (< 10 km horizontal resolution) many times per day (Key et al., 2012). Measurements from a mountaintop location, such as CLARS, provide similar spatial and temporal resolution as GEO measurements but with a larger viewing zenith angle which enhances the optical path in the planetary boundary layer. We also demonstrate simultaneous XCH_4 and XCO_2 measurements are essential to quantify megacity GHG emissions and also provide critical information from which to attribute emissions to different economic sectors.

2 Measurement technique

2.1 CLARS-FTS

A JPL-built Fourier Transform Spectrometer (FTS) has been deployed since 2010 at the CLARS facility on Mount Wilson at an altitude of 1670 m a.s.l. overlooking the Los Angeles megacity (Fig. 1). The FTS operates in two modes: the Spectralon Viewing

ACPD
14, 17037–17066, 2014

Observations (SVO) and the Los Angeles Basin Surveys (LABS). In the SVO mode, the FTS points at a Spectralon® plate placed immediately below the FTS telescope to quantify the total column CO_2 and CH_4 above the megacity (above 1670 m and the basin planetary boundary layer (PBL) height). The SVO measurements represent approximately free tropospheric background levels. In the LABS mode, the FTS points downward at 28 geographical points in the basin acquiring spectra from reflected sunlight in the near-infrared region (Table 1). Our measurement technique from Mount Wilson mimics satellite observations, which measure surface reflectance from space or atmospheric absorptions of GHGs along the optical path – (1) from the sun to the surface and (2) from the surface to the instrument. The locations of the reflection points are selected to provide the best coverage of the megacity (Fig. 1). In addition, reflection points are chosen with uniform surface albedo across the spectrometer field of view using a near infrared camera. Reflection points sample from the San Bernardino Mountains in the east to the Pacific coast in the west, and from the base of the San Gabriel Mountains in the north to Long Beach Harbor and Orange County in the south. For a typical PBL height, the geometric slant paths within the PBL range from ∼ 4 km (Santa Anita Park) to ∼ 39 km (Lake Mathews). The points in Table 1 are the baseline raster pattern, but can be modified easily if desired. In the standard measurement cycle, the FTS points at these 28 reflection points and performs four SVO measurements per cycle. There are 5–8 measurement cycles per day depending on the time of the year.

The spectral resolution used in the CLARS-FTS measurement is 0.12 cm^{-1}, with an angular radius of the field of view of 0.5 mrad. The footprints in the Los Angeles basin are ellipses with surface areas ranging from 0.04 to 21.62 km^2 (Table 1). The pointing calibration procedure is designed to maximize pointing accuracy (Fu et al., 2014). Pointing uncertainties are primarily due to errors arising from gimbal tilt and minor position-dependent flexing of the pointing system structure. After pointing calibration corrections are applied, the CLARS-FTS pointing system has a total uncertainty of 0.17° (1 sigma) in azimuth, which is about 30 % of the CLARS-FTS field of view. This

ACPD
14, 17037–17066, 2014

results in a ground distance error of about 60 m for a reflection point located 20 km from Mount Wilson. Uncertainty is 0.045° (1 sigma) in elevation, that is, 8 % of the CLARS-FTS field of view, resulting in a ground distance error of about 16 m for a target that is 20 km from Mount Wilson. Details concerning the CLARS-FTS design, operation and calibration are described in Fu et al. (2014).

2.2 Data processing

The CLARS interferogram processing program (CLARS-IPP) converts the recorded interferograms into spectra. The CLARS-IPP also corrects for solar intensity variations and phase error. 12 single scan spectra are co-added over a period of 3 min for each reflection point to achieve a spectral signal-to-noise ratio (SNR) of ~ 300 : 1 for LABS measurements and ~ 450 : 1 for SVO measurements. The instrument line shape (ILS) of the CLARS-FTS is characterized using an external lamp and an HCl gas cell. Our experiment works on a simple Beer-Lambert principle where the number densities of CO_2 and CH_4 are proportional to the optical depths measured for rotationally resolved near infrared absorption spectra. Slant column density (SCD), the total number of absorbing molecule per unit area along the sun-Earth-instrument optical path, is retrieved for CO_2 and CH_4 using a modified version of the GFIT algorithm (Wunch et al., 2011; Fu et al., 2014). Descriptions of the CLARS-FTS data processing and retrieval algorithm are included in Fu et al. (2014). In the present analysis, we retrieve CO_2 from bands at 1.6 µm, CH_4 at 1.67 µm, and O_2 at 1.27 µm. The retrieved SCDs are converted to slant column-averaged dry air mole fractions, XCO_2 and XCH_4, by normalizing to SCD_{O_2} (Eq. 1).

$$XGHG = \frac{SCD_{GHG}}{SCD_{O_2}} \times 0.2095 \quad (1)$$

This method has been shown to improve the precision of XCO_2 and XCH_4 retrievals since SCD_{O_2} retrieval effectively cancels out first-order path length, instrumental, and

ACPD
14, 17037–17066, 2014

retrieval algorithm errors (Washenfelder and Wennberg, 2003; Washenfelder et al., 2006; Wunch et al., 2011; Fu et al., 2014). Measurement precisions are 0.3 ppm for XCO_2 (~ 0.1 %) and 2.5 ppb for XCH_4 (~ 0.1 %) for the SVO measurements and 0.6 ppm for XCO_2 (~ 0.1 %) and 4.7 ppb for XCH_4 (~ 0.2 %) for the LABS measurements. Estimated measurement accuracies are < 3.1 % for XCO_2 and < 6.0 % for XCH_4, driven mainly by uncertainties in laboratory spectra line parameters.

2.3 Data filtering

Poor air quality in Los Angeles causes visibility reduction due to aerosol scattering. While the impact of aerosol scattering is significantly lower in the infrared than the visible and ultraviolet spectral regions, CLARS-FTS trace gas retrievals can be affected by aerosols due to the long optical path length in the boundary layer. In addition to aerosol, the Los Angeles megacity is often affected by morning marine layer fog and low clouds, which influence the data quality.

Individual retrievals are analyzed with multiple post-processing filters to ensure data quality, similar to the QA/QC filters adopted in the Atmospheric CO_2 observations from Space (ACOS) – GOSAT data processing (O'Dell et al., 2012; Crisp et al., 2012; Mandrake et al., 2013). Table 2 summarizes the filtering criteria. Data with poor spectral fitting quality, such as with large solar zenith angle (SZA), low SNR and/or large fitting residual root mean square errors (RMS), are removed. Data are also screened for clouds and aerosols using the ratio of retrieved to geometric oxygen SCDs as the criterion. The geometric oxygen SCD is calculated using surface pressure from National Center for Environmental Prediction (NCEP) reanalysis data assuming hydrostatic equilibrium, a constant oxygen dry-air volume mixing ratio of 0.2095 along the optical path and no scattering or absorption occurs (Fu et al., 2014). Because oxygen is well mixed in the atmosphere, deviations in the retrieved oxygen SCD from the geometric oxygen SCD indicate variations of the light path due to clouds and/or aerosols, assuming deviations are larger than the retrieval uncertainty, that is, < 0.3 % for SVO measurements and ~ 0.5 % for LABS measurements (errors represent precisions only). For

ACPD
14, 17037–17066, 2014

high clouds, data are filtered out when the corresponding SVO oxygen SCD ratio is less than 1 or greater than 1.1. For low clouds, data with retrieved target oxygen SCD deviating more than 10 % from the geometric value are removed. We use the same criteria to take out data with heavy aerosol loading which leads to significant modification in the light path. This filtering approach is equivalent to that used by ACOS, which compares the retrieved surface pressure to reanalysis data (O'Dell et al., 2012). As a result of our data filters, more data are removed for reflection points located further away from Mount Wilson since these measurements have larger fractions of their optical paths in the PBL and are more likely to encounter substantial scattering (Fig. 2).

Numerous studies have shown that aerosol scattering the atmosphere has an impact on the retrieved trace gas mixing ratios from space-based observations in the near-infrared (Aben et al., 2007; Yoshida et al., 2011; Crisp et al., 2012). Zhang et al. (2014) used a numerical two-stream radiative transfer model (RTM) validated against the VLIDORT full-physics RTM (Spurr et al., 2006) to estimate the expected biases in the retrieved values of XCO_2 and XCH_4 from CLARS observations. The model was used to set the value for the CLARS aerosol filter criterion in terms of the ratio of measured to geometric optical path length derived from the 1.27 µm absorption band of molecular oxygen (see section 4.1).

3 Observations

3.1 Diurnal variations of XCO_2 and XCH_4 : SVO vs. LABS

Due to the difference in the measurement geometry between the SVO mode and the LABS mode, the diurnal patterns of XCO_2 and XCH_4 differ significantly. Figure 3 shows an example of the diurnal variations of raw and filtered XCO_2 and XCH_4 measurements for the SVO mode, and the LABS west Pasadena and Santa Anita Park targets from ~ 08:30 to ~ 16:30 LT on seven continuous days during the period 5–11 May 2012. The SVO retrievals showed constant path-averaged mixing ratios of about 390 ppm XCO_2

ACPD
14, 17037–17066, 2014

and 1700 ppb XCH_4 during this period. The constant diurnal pattern was observed because the FTS is located most of the time above the planetary boundary layer where sources are located (Newman et al., 2013). Therefore the SVO measurements do not capture variations of atmospheric CO_2 and CH_4 mixing ratio due to emissions in the Los Angeles megacity.

On the other hand, the west Pasadena and Santa Anita Park reflection points exhibited strong diurnal signals in XCO_2 and XCH_4, with a minimum typically in the early morning of around 405–410 ppm for XCO_2 and 1800–1900 ppb for XCH_4 and a maximum of up to 420 ppm for XCO_2 and 1950 ppb for XCH_4 at noon or in the early afternoon. Variability in CO_2 and CH_4 emissions and atmospheric transport resulted in daily ranges of variation of 10–30 ppm XCO_2 and 100–200 ppb XCH_4 during the period of 5–11 May 2012. With a typical boundary layer height, the west Pasadena and the Santa Anita Park measurements sample horizontally over a few kilometers in the PBL and are therefore sensitive to emission signatures. The buildup of XCO_2 and XCH_4 in the morning and the falloff in the afternoon are due to a combination of accumulation of emissions and dilution/advection processes in basin. Similar diurnal patterns of XCO_2 and XCH_4 (that is, peak at noon or early afternoon) have been observed in Pasadena by a TCCON station (Wunch et al., 2009). However, the column enhancements observed by TCCON are typically less than 2–3 ppm in XCO_2 and 20–40 ppb in XCH_4. These enhancements are significantly smaller than those derived from the CLARS-FTS measurements which have a longer optical path within the PBL compared with TCCON at the same SZA.

Variations in PBL height do not affect the diurnal profiles of XCO_2 and XCH_4 as they would in in-situ measurements in which diurnal variation is often characterized by GHG concentration peaks in the morning and evening when the PBL is shallow and a minimum in midday when the PBL has grown (Newman et al., 2013). This is because XCO_2 and XCH_4 are derived from the slant column abundance along the CLARS-FTS optical paths. This is valid as long as the PBL height is below Mount Wilson. Since

ACPD
14, 17037–17066, 2014

the PBL typically locates below Mount Wilson (Newman et al., 2013), this is a major advantage of column measurements over in-situ measurements.

3.2 Slopes of derived $CH_4 : CO_2$ correlations

Several studies have reported strong correlations between CH_4 and CO_2 measured in the PBL in source regions (Peischl et al., 2013; Wennberg et al., 2012; Wunch et al., 2009; S. Newman, personal communication, 2014). Slopes of $CH_4 : CO_2$ correlation plots have been identified with local emission ratios for the two gases. Since the uncertainty in CH_4 emissions is considerably larger than that in CO_2 emissions, we may use the correlation slope to reduce the CH_4 emission uncertainties. In this study, we determined the spatial variation of $CH_4 : CO_2$ ratios originating from CLARS-FTS measurements between September 2011 and October 2013. It is first necessary to remove the background variations in CO_2 and CH_4 in order to calculate the concentration anomalies resulting from emissions in the PBL. Different approaches to deriving the background concentrations were considered including using the early morning, daily minimum and daily average XGHG for each reflection point. However, because of variations in the yield of LABS data passing through the data filters, biases may be introduced into the background estimation by these methods. As a result, we determined that the SVO observations, which have a very small diurnal variation, are the most appropriate background reference values for the CLARS LABS measurements. The excess XCO_2 and XCH_4 above background in the Los Angeles megacity are simply calculated by subtracting the SVO observations from the LABS observations (Eq. 2).

$$XGHG_{(XS)} = XGHG_{LABS} - XGHG_{SVO} \quad (2)$$

We used orthogonal distance regression (ODR) analysis of $XCH_{4(XS)}/XCO_{2(XS)}$ to quantify the emissions of CH_4 relative to CO_2 in the Los Angeles megacity. Using this approach, we find values of 7.3 ± 0.1 ppb CH_4 $(\text{ppm}\,CO_2)^{-1}$ for the west Pasadena reflection point and 6.1 ± 0.1 ppb CH_4 $(\text{ppm}\,CO_2)^{-1}$ for the Santa Anita Park reflection

ACPD
14, 17037–17066, 2014

point. Figure 4 illustrates the tight correlations found between $XCH_{4(XS)}$ and $XCO_{2(XS)}$ for each reflection point. The tight correlations imply that there is not substantial difference in the emission ratio of the two GHGs during the measurement period from 2011 to 2013. $XCH_{4(XS)}$ and $XCO_{2(XS)}$ should be poorly correlated with each other if their emission ratio varies largely over time, assuming the correlation is mainly driven by emissions.

Figure 5 maps the observed $XCH_{4(XS)}/XCO_{2(XS)}$ correlation slopes (in units of ppb CH_4 (ppm CO_2)$^{-1}$) across the Los Angeles megacity using natural neighbor interpolation (Sibson, 1981). The mean for all 28 reflection points was 6.4 ± 0.5 ppb CH_4 (ppm CO_2)$^{-1}$ with individual values ranging from 5.4 to 7.3 ppb CH_4 (ppm CO_2)$^{-1}$. Elevated $XCH_{4(XS)}/XCO_{2(XS)}$ ratios were observed in west Pasadena and in the eastern side of the Los Angeles megacity.

Spatial gradients among reflection points became weaker as distance from Mount Wilson increased. Stronger spatial gradients were observed among the closer reflection points in the basin, that is, west Pasadena, Santa Anita Park and East Los Angeles, while weaker spatial gradients were observed among the more distant reflection points, such as Long Beach, Marina Del Rey and North Orange County. Measurements were averaged over a much longer slant path for the more distant reflection points, compared to the nearby reflection points, making the measurements for the more distant reflection points less sensitive to local/point sources. Bootstrap analysis (Efron and Tibshirani, 1993) was performed to make sure that the spatial variations of the correlation slopes were not a result of sampling bias among the 28 reflection points. The uncertainties in the correlation slopes became larger with increasing distance from Mount Wilson due to the decreased data quality, as the measurement path in the Los Angeles megacity became longer. (More data were filtered out for targets further from the instrument, mostly because of aerosol loading.)

The CLARS-FTS observations in west Pasadena are in good agreement with TCCON measurements at the Jet Propulsion Laboratory, which showed a ratio of 7.8 ± 0.8 ppb CH_4 (ppm CO_2)$^{-1}$ (Wunch et al., 2009). Subtle differences between the

ACPD
14, 17037–17066, 2014

TCCON and the CLARS-FTS are to the relative change in the ratio over time, difference measurement geometry, and/or the different approach in determining the excess ratio. A number of in situ ground and aircraft measurements of CO_2 and CH_4 have been performed recently with the goal of quantifying GHG emissions in the megacity. A list of $CH_4 : CO_2$ ratios reported by these observations is shown in Table 4. These observations reported ratios ranging from 6.10 to 6.74 ppb CH_4 (ppm CO_2)$^{-1}$ (Wennberg et al., 2012; Peischl et al., 2013; S. Newman and Y.-K. Hsu, personal communication, 2014; Y.-K. Hsu, personal communication, 2014). Because of the different measurement techniques, measurement periods and locations, $CH_4 : CO_2$ ratios reported by these studies are not directly comparable to column measurements. However, the CLARS-FTS observations of $CH_4 : CO_2$ ratios show consistency with these measurements.

4 Discussion

4.1 Analysis assumptions

A number of assumptions are involved in deriving the $CH_4 : CO_2$ emission ratios. These are described in this subsection.

– $XCH_{4(XS)}$ and $XCO_{2(XS)}$ are correlated even though the two GHGs are not emitted from the same sources. CH_4 and CO_2 have chemical lifetimes that are much longer than the timescales for mesoscale transport and therefore behave like inert tracers in the boundary layer. Even if emitted from different sources, atmospheric processes in the boundary layer will result in mixing on relatively short timescales (typical mixing timescale in the PBL is on the order of 10–20 min, Stull, 1988). CLARS-FTS samples air masses that have undergone this short timescale mixing. The high degree of correlation observed between $XCH_{4(XS)}$ and $XCO_{2(XS)}$ for all 28 reflection points supports this mixing assumption over the entire area of the LA basin.

ACPD
14, 17037–17066, 2014

– The slope of the $XCH_{4(XS)} : XCO_{2(XS)}$ correlation observed at each LABS measurement point is sensitive to both the relative emissions over a horizontal path weighted toward the reflection point, and the composition of the air mass advected into the atmospheric path. The long optical path in the boundary layer and the effect of advection smear out the effects of local emission ratio variations. This smearing is different for each reflection point. Future work will deconvolve these effects using an atmospheric transport model which will include advection, boundary layer mixing, surface emissions and ray-tracing of the optical path sampled by CLARS-FTS on a 1–2 km grid.

– The effect of aerosol scattering on the $XCH_{4(XS)} : XCO_{2(XS)}$ slopes is assumed to be negligible. Using a two-stream numerical radiative transfer model constrained by AERONET aerosol optical depths in the near-infrared, Zhang et al. (2014) showed that the bias in the retrieved XCO_2 from CLARS-FTS LABS measurements does not exceed 1 %, using data that have passed the filter criteria described above. This bias is caused by the wavelength dependence of aerosol scattering and absorption between the CO_2 absorption band at 1.61 µm, and the O_2 absorption band at 1.27 µm. Since the CO_2 and CH_4 observations used in this analysis are retrieved at nearly identical wavelengths (1.61 µm vs. 1.66 µm), the aerosol-induced bias on XCO_2 and XCH_4 should be nearly identical and cancel out in the ratio. Uncertainties due to aerosol scattering on the CLARS-FTS XCO_2 and XCH_4 observations will be reduced significantly in the next version of the CLARS-FTS retrieval algorithm which will consider aerosol scattering explicitly in the forward model (Zhang et al., 2014).

– The number of discrete reflection points (28 plus the direct solar path) is sufficient to characterize the average emission ratio over the Los Angeles megacity. The CLARS-FTS LABS mode spans slant distances in the range 4–40 km in the Los Angeles PBL, and therefore should have sufficient spatial coverage of the megacity. In the future, sensitivity studies will be performed to optimize the spatial

ACPD
14, 17037–17066, 2014

distribution of the reflection points with respect to coverage of emission sources, aerosol bias, albedo variability, locations of other stations in the monitoring network, and other parameters.

– Averaging the monthly average XCH_4/XCO_2 ratio over a two-year period to derive annual average CH_4 emissions does not introduce a temporal sampling bias. Certain times of the year are more likely to be influenced by cloud and aerosol events in Los Angeles and have correspondingly fewer measurements that pass the data quality filters. In our analysis the effect of seasonal bias is assumed to small. Since good correlation is observed between $XCH_{4(XS)} : XCO_{2(XS)}$ throughout the year, the contribution of seasonal sampling bias, if any, has a negligible effect on the random error of the annual average $XCH_{4(XS)} : XCO_{2(XS)}$ correlation slope.

4.2 Top-down CH_4 emissions from CLARS-FTS observations

With the assumptions described in the previous subsection, we estimate the top-down annual CH_4 emission for the Los Angeles megacity based on the CLARS-FTS observations. The CARB reported an annual statewide CO_2 emission of 387 Tg CO_2 year^{-1} for 2011 (California Air Resources Board, http://www.arb.ca.gov/app/ghg/2000_2011/ghg_sector.php). Since the majority of CO_2 emissions are from fossil fuel combustion, we assumed that the CO_2 emissions are spatially distributed by population in the state. We apportioned the statewide emissions by population in the Los Angeles megacity, which is 43 % of statewide population, to estimate the bottom-up emission for the Los Angeles megacity (http://www.census.gov/). The bottom-up CO_2 emission inventory for the Los Angeles megacity was thus 166 ± 23 Tg CO_2 year^{-1} in 2011, assuming 10 % uncertainties in both the CARB statewide CO_2 emission and the spatial distribution of emissions by population. For the bottom-up CH_4 emission in the Los Angeles megacity, we used the same method as in Wunch et al. (2009) and Peischl et al. (2013). That is, subtracting agriculture and forestry sector from the total statewide emission, then

ACPD
14, 17037–17066, 2014

apportioned by population. This gave a bottom-up CH_4 emission inventory of 0.28 Tg CH_4 $year^{-1}$ in the Los Angeles megacity in 2011. Using the bottom-up emission inventory of CO_2 for the Los Angeles megacity and the $CH_4 : CO_2$ ratio observed by the CLARS-FTS, we derived the CH_4 emission inventory using Eq. (3), where $E_{CH_4}|_{top\text{-}down}$ is the top-down CH_4 emissions inferred by the CLARS-FTS observations, $E_{CO_2}|_{bottom\text{-}up}$ is the bottom-up CO_2 emissions, $\frac{XCH_4}{XCO_2}|_{slope}$ is the $XCH_{4(XS)}/XCO_{2(XS)}$ ratio observed by the FTS and $\frac{MW_{CO_2}}{MW_{CH_4}}$ is the ratio of molecular weight of CO_2 and CH_4.

$$E_{CH_4}|_{top\text{-}down} = E_{CO_2}|_{bottom\text{-}up} \times \frac{XCH_4}{XCO_2}|_{slope} \times \frac{MW_{CH_4}}{MW_{CO_2}} \quad (3)$$

The derived CH_4 emission inventory was 0.39 ± 0.06 Tg CH_4 $year^{-1}$ in the Los Angeles megacity assuming a 10 % uncertainty in the CARB bottom-up CO_2 emission. The derived CH_4 emission inventory was 18–61 % larger than the bottom-up emission inventory in 2011. This is in good agreement with recent studies (Wunch et al., 2009; Hsu et al., 2010; Wennberg et al., 2012; Peischl et al., 2013; Jeong et al., 2013).

Because of the spatial and temporal variations of $CH_4 : CO_2$ ratio in the Los Angeles megacity, the derived CH_4 emission based on local observations can be biased. For instance, if we were to evaluate the bottom-up CH_4 emission inventory by our observations in west Pasadena only, the derived CH_4 emission inventory for the Los Angeles megacity would be overestimated by 14 %, since the west Pasadena target observed a $CH_4 : CO_2$ slope that is 14 % larger than the average slope of the 28 reflection points. Therefore, to quantify and to reduce uncertainties in carbon emissions from the Los Angeles megacity or any other urban areas which are highly heterogeneous, it is important to have measurements which provide both spatial and temporal coverage. It is challenging to quantify individual point sources of CH_4. Further investigations need to be performed to link the CLARS-FTS observations to emissions from landfills, oil extraction and natural gas pipeline leakage.

ACPD
14, 17037–17066, 2014

4.3 Relevance to future satellite GHG observations

This study has shown that spatially resolved $CH_4 : CO_2$ emission ratio measurements can be made over a megacity domain (hundreds of km^2) using a remote sensing method that simulates the observations from an imaging spectrometer such as GEO-FTS from geostationary orbit. From GEO, the field of regard is approximately one-third of the Earth below 60°. latitude. Operating as a hosted payload from a commercial communications satellite, measurements of XCO_2, XCH_4, XCO and solar-induced chlorophyll fluorescence (SIF) will be made every 1–2 h during daylight with a pixel footprint of 2–3 km at the sub-satellite point with retrieval precisions comparable to those obtained from CLARS-FTS (Fu et al., 2014). In the near future, a two-dimensional imaging FTS similar to GEO-FTS will be deployed at CLARS to increase the spatial density of the retrievals.

5 Conclusions

This study is the first to map GHGs in the Los Angeles megacity using ground-based remote sensing technique. It combines the unique vista from Mount Wilson and high-sensitivity measurements made by the CLARS-FTS to simulate satellite observations. Persistent space and time resolved observations of GHG in the Los Angeles megacity over a two-year period in 2011–2013 and a tracer-to-tracer correlation analysis are used to reveal interesting spatial pattern of $CH_4 : CO_2$ ratio in the megacity. The slope of the correlations between $XCH_{4(XS)}$ and $XCO_{2(XS)}$ showed significant spatial variations ranging from 5.4 to 7.3 ppb CH_4 $(\text{ppm } CO_2)^{-1}$, with an average of 6.4 ± 0.5 ppb CH_4 $(\text{ppm } CO_2)^{-1}$, indicating that there is spatial heterogeneity in the megacity. Using the CARB bottom-up emission inventory of CO_2, we derived the CH_4 emission inventory of the Los Angeles megacity in 2011–2013 to be 0.39 ± 0.06 Tg CH_4 year^{-1}, which was 18–61 % above the bottom-up CH_4 emission inventory. Good agreements among previous aircraft observations and local observations indicated the CLARS-FTS to be

ACPD
14, 17037–17066, 2014

a robust measurement technique that can quantify and track GHG emissions in the Los Angeles megacity in an efficient way. The CLARS-FTS also demonstrates the potential success for future satellite mission to quantify carbon emissions from megacities from space. The heterogeneity characteristics in the megacity can lead to a 14 % uncertainty in the derived top-down CH_4 emissions if only observations in west Pasadena are used. However, due to the complexity of the measurement geometry of the CLARS-FTS observations, it is challenging to pinpoint local sources or to derive a map of local $CH_4 : CO_2$ emission ratios at this point. Additional future work needs to be done. The CLARS-FTS observations, which span the Los Angeles megacity continuously, fill the gap between the local measurements that provide long-term observations but are too sensitive to local emissions, and aircraft data that provides intense spatial and temporal observations yet are too expensive to carry out continuously throughout the year. However, it is necessary to combine the CLARS-FTS observations with in-situ ground and aircraft data for a long-term GHG monitoring effort in the megacity.

Acknowledgements. The authors thank our colleagues and D. Wunch (California Institute of Technology), J. Stutz (University of California, Los Angeles) and G. Keppel-Aleks (University of Michigan) for helpful comments. Support from the California Air Resources Board, NOAA Climate Program, NIST GHG and Climate Science Program and JPL Earth Science and Technology Directorate is gratefully acknowledged. Y. L. Yung, was supported in part by NASA grant NNX13AK34G to the California Institute of Technology and the KISS program of Caltech.

References

Aben, I., Hasekamp, O., and Hartmann, W.: Uncertainties in the space-based measurements of CO_2 columns due to scattering in the Earth's atmosphere, J. Quant. Spectrosc. Ra., 104, 450–459, 2007.

Crisp, D., Fisher, B. M., O'Dell, C., Frankenberg, C., Basilio, R., Bösch, H., Brown, L. R., Castano, R., Connor, B., Deutscher, N. M., Eldering, A., Griffith, D., Gunson, M., Kuze, A., Mandrake, L., McDuffie, J., Messerschmidt, J., Miller, C. E., Morino, I., Natraj, V., Notholt, J., O'Brien, D. M., Oyafuso, F., Polonsky, I., Robinson, J., Salawitch, R., Sherlock, V., Smyth, M.,

ACPD
14, 17037–17066, 2014

Suto, H., Taylor, T. E., Thompson, D. R., Wennberg, P. O., Wunch, D., and Yung, Y. L.: The ACOS CO_2 retrieval algorithm – Part II: Global XCO_2 data characterization, Atmos. Meas. Tech., 5, 687–707, doi:10.5194/amt-5-687-2012, 2012.

Efron, B. and Tibshirani, R.: An Introduction to the Bootstrap, Vol. 57, CRC press, Boca Raton, Florida, USA, 1993.

Fu, D., Pongetti, T. J., Blavier, J.-F. L., Crawford, T. J., Manatt, K. S., Toon, G. C., Wong, K. W., and Sander, S. P.: Near-infrared remote sensing of Los Angeles trace gas distributions from a mountaintop site, Atmos. Meas. Tech., 7, 713–729, doi:10.5194/amt-7-713-2014, 2014.

Hsu, Y.-K., VanCuren, T., Park, S., Jakober, C., Herner, J., FitzGibbon, M., Blake, D. R., and Parrish, D. D.: Methane emissions inventory verification in southern California, Atmos. Environ., 44, 1–7, 2010.

Jeong, S., Hsu, Y.-K., Andrews, A. E., Bianco, L., Vaca, P., Wilczak, J. M., and Fischer, M. L.: A multitower measurement network estimate of California's methane emissions, J. Geophys. Res.-Atmos., 118, 11339–11351, doi:10.1002/jgrd.50854, 2013.

Key, R., Sander, S., Eldering, A., Blavier, J-F, Bekker, D., Manatt, K., Rider, D., and Wu, Y.-H.: The geostationary fourier transform spectrometer, Proc. SPIE, 8515, doi:10.1117/12.930257, 2012.

Kort, E. A., Angevine, W. M., Duren, R., and Miller, C. E.: Surface observations for monitoring urban fossil fuel CO_2 emissions: Minimum site location requirements for the Los Angeles megacity, J. Geophys. Res.-Atmos., 118, 1577–1584, doi:10.1002/jgrd.50135, 2013.

Mandrake, L., Frankenberg, C., O'Dell, C. W., Osterman, G., Wennberg, P., and Wunch, D.: Semi-autonomous sounding selection for OCO-2, Atmos. Meas. Tech., 6, 2851–2864, doi:10.5194/amt-6-2851-2013, 2013.

Newman, S., Jeong, S., Fischer, M. L., Xu, X., Haman, C. L., Lefer, B., Alvarez, S., Rappenglueck, B., Kort, E. A., Andrews, A. E., Peischl, J., Gurney, K. R., Miller, C. E., and Yung, Y. L.: Diurnal tracking of anthropogenic CO_2 emissions in the Los Angeles basin megacity during spring 2010, Atmos. Chem. Phys., 13, 4359–4372, doi:10.5194/acp-13-4359-2013, 2013.

O'Dell, C. W., Connor, B., Bösch, H., O'Brien, D., Frankenberg, C., Castano, R., Christi, M., Eldering, D., Fisher, B., Gunson, M., McDuffie, J., Miller, C. E., Natraj, V., Oyafuso, F., Polonsky, I., Smyth, M., Taylor, T., Toon, G. C., Wennberg, P. O., and Wunch, D.: The ACOS CO_2 retrieval algorithm – Part 1: Description and validation against synthetic observations, Atmos. Meas. Tech., 5, 99–121, doi:10.5194/amt-5-99-2012, 2012.

ACPD
14, 17037–17066, 2014

Peischl, J., Ryerson, T. B., Brioude, J., Aikin, K. C., Andrews, A. E., Atlas, E., Blake, D., Daube, B. C., de Gouw, J. A., Dlugokencky, E., Frost, G. J., Gentner, D. R., Gilman, J. B., Goldstein, A. H., Harley, R. A., Holloway, J. S., Kofler, J., Kuster, W. C., Lang, P. M., Novelli, P. C., Santoni, G. W., Trainer, M., Wofsy, S. C., and Parrish, D. D.: Quantifying sources of methane using light alkanes in the Los Angeles basin, California, J. Geophys. Res.-Atmos., 118, 4974–4990, doi:10.1002/jgrd.50413, 2013.

Sibson, R.: A brief description of natural neighbor interpolation, in: Interpreting Multivariate Data, edited by: Barnet, V., Wiley, Chichester, 21–36, 1981.

Spurr, R. J: VLIDORT: A linearized pseudo-spherical vector discrete ordinate radiative transfer code for forward model and retrieval studies in multilayer multiple scattering media, J. Quant. Spectrosc. RA., 102, 2, 316–342, 2006.

Stull, R: An Introduction to Boundary Layer Meteorology, Springer, the Netherlands, 1988.

Washenfelder, R. A. and Wennberg, P. O.: Tropospheric methane retrieved from ground-based near-IR solar absorption spectra, Geophys. Res. Lett., 30, 23, 2226, doi:10.1029/2003GL017969, 2003.

Washenfelder, R. A., Toon, G. C., Blavier, J.-F., Yang, Z., Allen, N. T., Wennberg, P. O., Vay, S. A., Matross, D. M., and Daube, B. C.: Carbon dioxide column abundances at the Wisconsin Tall Tower site, J. Geophys. Res., 111, D22305, doi:10.1029/2006JD007154, 2006.

Wennberg, P. O., Mui, W., Wunch, D., Kort, E. A., Blake, D. R. Atlas, E. L., Santoni, G. W., Wofsy, S. C., Diskin, G. S., Joeng, S., and Fischer, M. L.: On the sources of methane to the Los Angeles atmosphere, Environ. Sci. Technol., 46, 9282–9289, doi:10.1021/es301138y, 2012.

Wunch, D., Wennberg, P. O.,Toon, G. C., Keppel-Aleks, G., and Yavin, Y. G.: Emissions of greenhouse gases from a North American megacity, Geophys. Res. Lett., 36, L15810, doi:10.1029/2009GL039825, 2009.

Wunch, D., Toon, G. C., Blavier, J. L., Washenfelder, R. A., Notholt, J., Connor, B. J., Griffith, D. W., Sherlock, V., and Wennberg, P. O.: The total carbon column observing network, Philos. T. Roy. Soc. A, 369, 2087–2112, 2011.

Yoshida, Y., Ota, Y., Eguchi, N., Kikuchi, N., Nobuta, K., Tran, H., Morino, I., and Yokota, T.: Retrieval algorithm for CO_2 and CH_4 column abundances from short-wavelength infrared spectral observations by the Greenhouse Gases Observing Satellite, Atmos. Meas. Tech., 4, 4, 717–734, 2011.

ACPD
14, 17037–17066, 2014

Zhang, Q., Natraj, V., Li, K., Shia, R., Fu, D., Pongetti, T., Sander, S. P., and Yung, Y. L.: Influence of aerosol scattering on the retrieval of CO_2 mixing ratios: a case study using measurements from the California Laboratory for Atmospheric Remote Sensing (CLARS), Geophys. Res. Lett., in preparation, 2014.

California Air Resources Board: Greenhouse gas emission inventory – Query tool for years 2000 to 2011, 6th Edn., http://www.arb.ca.gov/app/ghg/2000_2011/ghg_sector.php, last access: January 2014.

ACPD

14, 17037–17066, 2014

Table 1. List of the 29 reflection points on Mount Wilson and in the Los Angeles megacity.

	Target	Latitude	Longitude	Slant distance from FTS (km)	*Slant path in PBL (km)	Footprint (km^2)
1	Spectralon®, Mount Wilson	34.22	−118.06	0.01	0	0
2	Santa Anita Park	34.14	−118.04	9.2	4.2	0.04
3	west Pasadena	34.17	−118.17	11.5	5.9	0.09
4	Santa Fe Dam	34.11	−117.97	14.9	6.8	0.17
5	East Los Angeles	34.05	−118.12	20.2	9.2	0.41
6	Fwy 210	34.12	−117.87	20.9	10.1	0.49
7	Downtown (near)	34.10	−118.23	21.1	9.6	0.47
8	Glendale	34.15	−118.27	21.4	10.0	0.50
9	Fwys 60 and 605	34.03	−118.03	21.7	9.5	0.49
10	Universal City	34.14	−118.35	28.8	13.4	1.23
11	Fwy 60, City of Industry	34.00	−117.88	29.6	13.7	1.33
12	Downtown (far)	34.05	−118.31	29.7	12.9	1.25
13	Downey	33.93	−118.16	33.9	14.5	1.84
14	La Mirada	33.91	−118.01	35.2	15.3	2.09
15	Pomona	34.04	−117.73	36.7	18.1	2.70
16	Santa Monica Mountains	34.09	−118.47	40.9	20.2	3.74
17	Marina Del Rey	33.99	−118.40	41.0	17.3	3.22
18	Rancho Cucamonga	34.08	−117.59	46.1	24.0	5.66
19	Long Beach	33.82	−118.20	46.5	19.6	4.70
20	North Orange County	33.86	−117.78	47.8	21.3	5.38
21	Angels Stadium	33.80	−117.88	49.8	21.5	5.89
22	Norco	33.96	−117.57	53.5	25.3	8.01
23	Palos Verdes	33.81	−118.37	54.2	23.7	7.70
24	Huntington Beach	33.72	−117.98	56.2	23.8	8.32
25	Corona	33.87	−117.60	56.0	28.8	10.71
26	Orange Country Airport	33.68	−117.86	63.3	26.7	11.86
27	Fontana	34.07	−117.39	64.3	33.8	15.46
28	Riverside	33.95	−117.39	68.5	34.1	17.75
29	Lake Mathews	33.88	−117.42	70.7	39.1	21.62

* Slant paths in PBL are estimated assuming a uniform PBL height of 700 m, which was the average PBL height observed during CalNex 2010.

ACPD
14, 17037–17066, 2014

Table 2. Data filter criteria.

Filter	Criteria
High clouds	SVO $O_{2\ SCD\_retrieved} : O_{2\ SCD\_Geometric} > 1.1$ or < 1
Low clouds and/or aerosol	LABS $O_{2\ SCD\_retrieved} : O_{2\ SCD\_geometric} > 1.1$ or < 0.9
Large SZA	SZA $> 70^{\circ}$
Low SNR	SNR < 100
Poor spectral fitting	Fitting residual RMS > 1 standard deviation above average

ACPD
14, 17037–17066, 2014

Table 3. List of correlation slopes of $XCH_{4(XS)} : XCO_{2(XS)}$ and their uncertainties (one standard deviation) observed by the CLARS-FTS between the period of September 2011 and October 2013.

Target	$XCH_{4(xs)}/XCO_{2(xs)}$ (ppb/ppm)	Uncertainties (ppb/ppm)
Santa Anita Park	6.09	0.05
west Pasadena	7.28	0.09
Santa Fe Dam	5.85	0.12
East Los Angeles	5.99	0.15
Fwy 210	6.26	0.20
Downtown (near)	6.42	0.21
Glendale	6.04	0.20
Fwys 60 and 605	7.34	0.31
Universal City	6.47	0.28
Fwy 60, City of Industry	7.25	0.41
Downtown (far)	6.33	0.23
Downey	6.24	0.29
La Mirada	7.13	0.35
Pomona	6.52	0.25
Santa Monica Mountains	6.55	0.33
Marina Del Rey	6.75	0.27
Rancho Cucamonga	5.35	0.15
Long Beach	6.18	0.28
North OC	6.41	0.35
Angels Stadium	6.65	0.39
Norco	6.87	0.31
Palos Verdes	6.59	0.34
Huntington Beach	6.10	0.24
Corona	6.40	0.30
Orange Country Airport	5.99	0.29
Fontana	6.18	0.23
Riverside	6.40	0.32
Lake Mathews	5.99	0.23

ACPD
14, 17037–17066, 2014

Table 4. Comparisons of $CH_4 : CO_2$ ratios and derived top-down CH_4 emissions among various measurements in the Los Angeles megacity. Please note that it is difficult to compare the uncertainties due to the different measurement techniques.

Measurement (Location, period)	$CH_4 : CO_2$ ratio (ppb:ppm)	Derived top-down CH_4 emission ($Tg\,CH_4\,year^{-1}$)	Measurement type	References
TCCON (Pasadena, Aug 2007–Jun 2008)	7.80 ± 0.80	0.40 ± 0.10 0.60 ± 0.10	Column (FTS)	Wunch et al. (2009)
ARCTAS (LA, Jun 2008)	6.74 ± 0.58	0.47 ± 0.10	Aircraft in-situ (Picarro)	Wennberg et al. (2012)
CalNex (LA, May 2010–Jun 2010)	6.70 ± 0.01	0.41 ± 0.04	Aircraft in-situ (Picarro)	Peischl et al. (2013)
Caltech (Pasadena, Feb 2012–Aug 2012)	6.30 ± 0.01	0.38 ± 0.05	Surface in-situ	This study
Mount Wilson (Pasadena, Sep 2011–Jun 2013)	6.10 ± 0.10	0.37 ± 0.05	Surface in-situ (Picarro)	This study
CLARS-FTS, Mount Wilson (LA, Sep 2011–Oct 2013)	6.40 ± 0.50	0.39 ± 0.06	Column (FTS)	This study

ACPD
14, 17037–17066, 2014

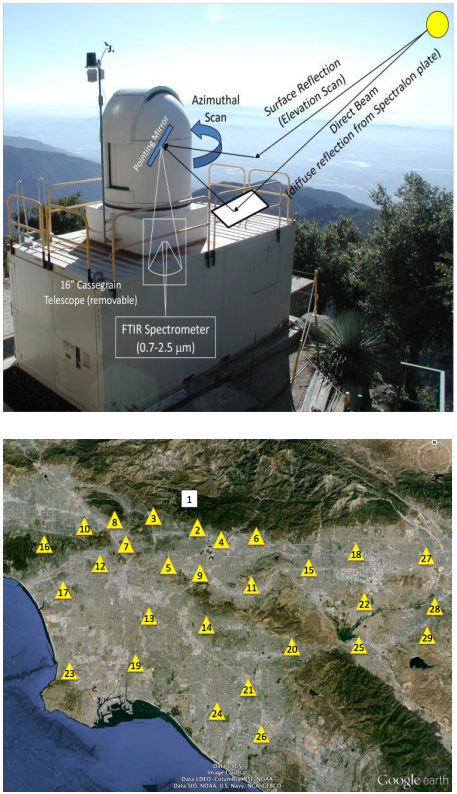

Figure 1. The CLARS-FTS on Mount Wilson (top) and its 29 reflection points on Mount Wilson and in the Los Angeles megacity (bottom). Reflection points are labeled in the order of increasing distance from the FTS. Information of the reflection points is given in Table 1. A small fraction of the central Los Angeles megacity area cannot be viewed from Mount Wilson due to a nearby mountain peak.

ACPD
14, 17037–17066, 2014

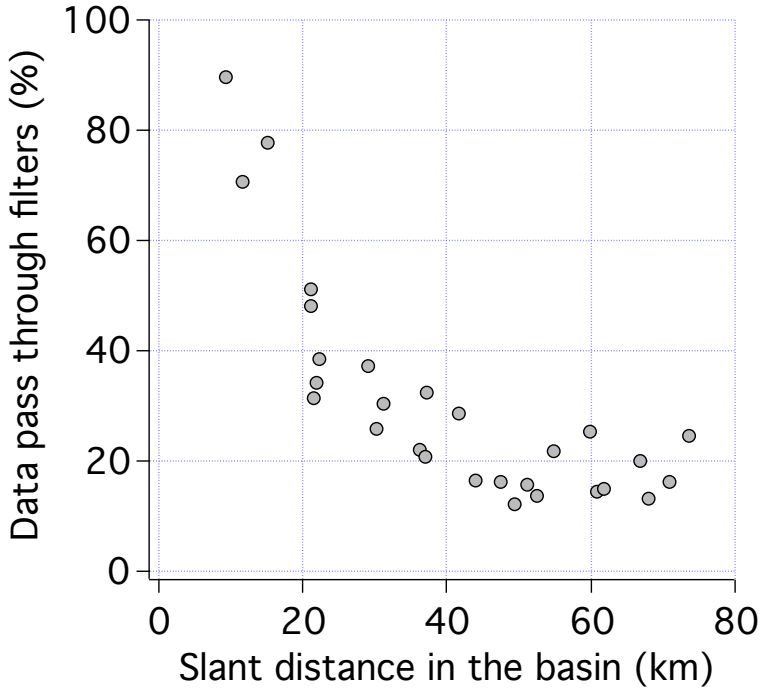

Figure 2. Percent of data points that pass through our data filters as a function of slant distance in the Los Angeles megacity.

ACPD
14, 17037–17066, 2014

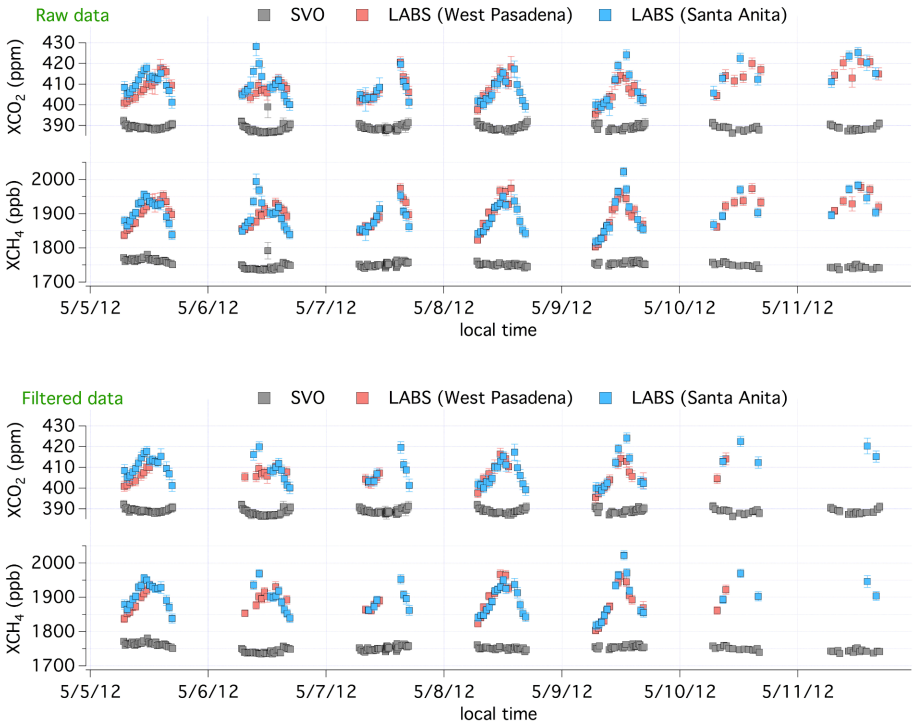

Figure 3. Upper panel shows the raw data and bottom panel shows the filtered data. Diurnal variations of SVO (grey) and LABS, west Pasadena (red) and Santa Anita Park (blue), XCO_2 and XCH_4 from around 08:30 to 16:30 local time (PST) on seven consecutive days in May 2012. Error bars represent the RMS of the retrieval spectral fitting residual. Bad data points, such as data taken in the cloudy morning of 11 May, were removed from the filtered data set. From 5–9 May, the FTS was operated in the target mode, taking alternate measurements among SVO, west Pasadena and Santa Anita Park. On 10–11 May, standard measurement cycle was performed, resulting in fewer measurements from each target.

ACPD
14, 17037–17066, 2014

Mapping $CH_4 : CO_2$ ratios in Los Angeles with CLARS-FTS from Mount Wilson, California

K. W. Wong et al.

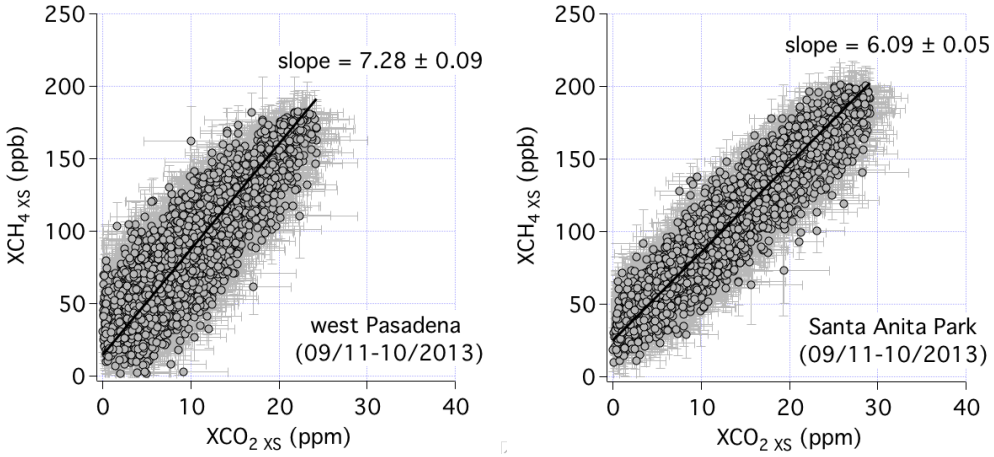

Figure 4. Correlations between $XCH_{4(XS)}$ (ppb) and $XCO_{2(XS)}$ (ppm) for west Pasadena and Santa Anita Park between the period of September 2011 and October 2013.

ACPD
14, 17037–17066, 2014

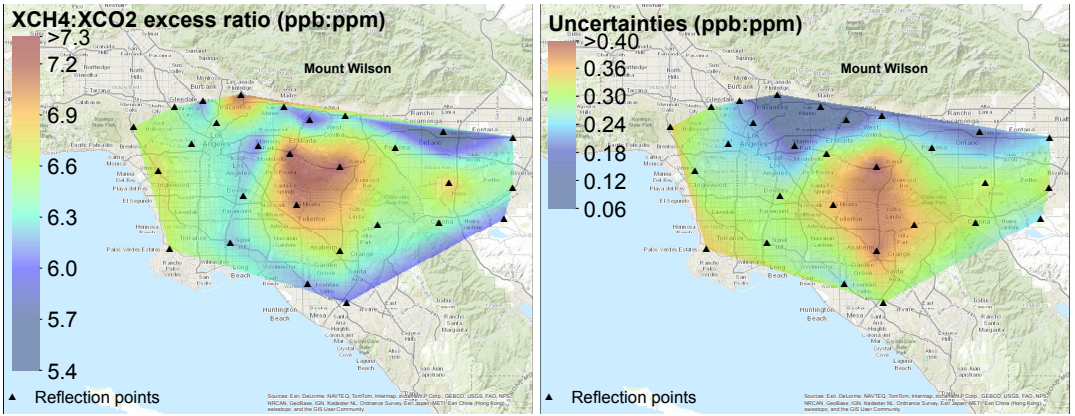

Figure 5. Maps of correlation slopes of $XCH_{4(XS)} : XCO_{2(XS)}$ (top) and their uncertainties (one standard deviation) (bottom) in the Los Angeles megacity observed by the CLARS-FTS between the period of September 2011 and October 2013. Sources: Esri, DeLorme, NAVTEQ, TomTom, Intermap, increment P Corp., GEBCO, USGS, FAO, NPS, NRCAN, GeoBase, IGN, Kadaster NL, Ordnance Survey, Esri Japan, METI, Esri China (Hong Kong), swisstopo, and the GIS User Community.

ACPD
14, 17037–17066, 2014

Mapping $CH_4 : CO_2$ ratios in Los Angeles with CLARS-FTS from Mount Wilson, California

K. W. Wong et al.